RAA 2020 Vol. **20** No. **4**, 52(12pp) doi: 10.1088/1674–4527/20/4/52

http://www.raa-journal.org *http://iopscience.iop.org/raa*

***R**esearch in*
***A**stronomy and*
***A**strophysics*

Investigation of near-contact semi-detached binary W UMi through observations and evolutionary models

Faruk Soydugan, Esin Soydugan and Fahri Aliçavuş

Çanakkale Onsekiz Mart University, Faculty of Arts and Sciences, Department of Physics, 17020, Çanakkale, Turkey; *fsoydugan@comu.edu.tr*
Çanakkale Onsekiz Mart University, Astrophysics Research Center and Ulupınar Observatory, 17020, Çanakkale, Turkey

Received 2019 October 17; accepted 2019 December 2

Abstract W UMi is a near contact, semi-detached, double-lined eclipsing binary star with an orbital period of 1.7 d. Simultaneous analysis of new BVR multi-color light curves and radial velocity data yields the main astrophysical parameters of the binary and its component stars. We determined mass and radius to be $M_1 = 3.22 \pm 0.08\,M_\odot$, $R_1 = 3.63 \pm 0.04\,R_\odot$ for the primary star and $M_2 = 1.44 \pm 0.05\,M_\odot$, $R_2 = 3.09 \pm 0.03\,R_\odot$ for the secondary star. Based on analysis of mid-eclipse times, variation in the orbital period is represented by a cyclic term and a downward parabola. Mass loss from the system is suggested for a secular decrease ($-0.02\ \mathrm{s\,yr^{-1}}$) in the period. Both the mechanisms of a hypothetical tertiary star orbiting around W UMi and the surface magnetic activity of the less massive cooler companion were used to interpret periodic changes. Observational parameters were found to be consistent with binary stellar evolution models produced in the non-conservative approach of MESA at a higher metallicity than the Sun and an age of about 400 Myr for the system. Evidence that the system is rich in metal was obtained from spectral and kinematic analysis as well as evolution models. W UMi, a high mass ratio system compared to classical semi-detached binaries, is an important example since it is estimated from binary evolutionary models that the system may reach its contact phase in a short time interval.

Key words: binaries: eclipsing — stars: fundamental parameters — stars: evolution — stars: individual: W UMi

1 INTRODUCTION

In the field of astrophysics, the role and importance of double-lined eclipsing binaries (EBs) is well known. EBs provide accurate determination of absolute parameters, mainly the radius and mass of the components from simultaneous analysis of light and radial velocity (RV) curve data. Moreover, they are good indicators of distance.

Semi-detached Algol-type binaries (SDBs) consist of a less massive, sub-giant or giant secondary component of F-G-K spectral type and a hotter, more massive, main-sequence primary component which is B-A spectral type. In this type of EB, the secondary companion, which fills its Roche lobe, can display the loss of angular momentum and mass transfer to the more massive companion. In long period Algols with orbital periods (P) longer than $5-6$ d, we can expect a permanent accretion disk because of the accretion structure of the primary component (Kaitchuck & Honeycutt 1982). On the other hand, Algols with periods of $P < 3-4$ d show temporary weak accretion structures or evidence of a mass transfer process cannot be observed. SDBs are important because they display meaningful astrophysical processes and are useful for studying binary star evolution when taking into account the effects of mass transfer and loss.

Near-contact binaries (NCBs) are within the intermediate class according to Roche classification (Shaw 1994). SDBs may be also a member of SD2-type of NCBs, if the massive companions are very close to their inner Roche lobes (Zhu & Qian 2009). NCBs can be investigated to examine the evolutionary process of a possible transition from detached binary to semi-detached binary, and also from semi-detached binary to contact binary. In this study,

semi-detached binary W UMi is an SD2 type NCB candidate system.

W UMi (HIP 79069, BD+86 244, SAO 2692), a classical Algol-type binary system with an orbital period of about 1.701 d, was discovered by Astbury (1913). The first spectroscopic study of W UMi was carried out by Joy & Dustheimer (1935) who measured the RV values associated with only the primary component and estimated the spectral type to be A4 for the component. In a later spectroscopic study by Sahade (1945), because of determining lines belonging only to the hotter primary component, W UMi was again classified as a single line spectroscopic binary. Recently, Park et al. (2018) presented a spectroscopic and photometric study, which includes RVs of the primary and secondary stars and an orbital solution of the system.

UBV light curves (LCs) of W UMi were acquired by Devinney et al. (1970) and solved by the Russell-Merrill method. The same photometric data were re-analyzed by Mardirossian et al. (1980). Recent analysis of the LCs for the system was reported by Park et al. (2018), in which the mass ratio (q) of the components was determined and considered to be $q = 0.399$. In addition, the temperature of the massive star was found to be 9300±90 K using spectral analysis (Park et al. 2018). Therefore, the basic astrophysical parameters in that study were estimated as different from previous studies (e.g. Mardirossian et al. 1980; Djurašević et al. 2003). Payne-Gaposchkin (1952) firstly reported changes in the orbital period of the target. Orbital period variations of W UMi were interpreted as being in continuous decrease and also experiencing sudden changes as a result of mass loss by Nakamura et al. (1998). Lastly, Kreiner et al. (2008) announced a decrease and also a cyclic variation in the period. The cyclic changes were interpreted with a probable third body in the system specified as an M dwarf star.

The present study presents an analysis of new photometric and spectroscopic data and also the evolutionary status of W UMi, taking into account binary effects. Section 2 includes information on photometric and spectroscopic observations. RV values of the companions, properties of the system's orbit, and also the model atmosphere application are given in Section 3. Simultaneous analysis of the photometric multi-color LCs and RV data of the components are reported in Section 4. In the next section, we focus on probable factors causing variations in the period of the target. The following section includes the main astrophysical properties of the components and also evolutionary scenarios for W UMi. Finally, a discussion about the results and conclusions is presented.

2 PHOTOMETRIC AND SPECTROSCOPIC OBSERVATIONS

The differential BVR LCs of W UMi were observed during April – May 2012 on nine nights at the Observatory of Çanakkale Onsekiz Mart University using the 30-cm diameter Schmidt-Cassegrain telescope with an STL-1001E camera. We chose GSC 4655–00320 ($V = 9^{\rm m}.79$) and GSC 4651–00275 ($V = 11^{\rm m}.03$) as the comparison and check stars respectively, and no light changes were indicated for these stars during observations. We reduced the CCD frames obtained from each night's observation employing C-Munipack code (`http://integral.sci.muni.cz/`). The mean errors were calculated as about $0^{\rm m}.01$ for all filters. The initial epoch T_0 (HJD) = 2452500.3960 and orbital period $P = 1.7011371$ d taken from Kreiner (2004) were applied to calculate the orbital phases in the LCs.

Spectroscopic data of the target were acquired with a 0.91 m diameter telescope equipped with an eć helle spectrograph (FRESCO) at Catania Astrophysical Observatory. FRESCO has a resolving power of about about 20 000 Å. A CCD camera with 1024×1024 pixels (size 24×24 μm) with a thinned back illuminated SITe was utilized. The spectral data were recorded in 19 orders from about 4300 to 6650 Å. Signal to noise ratio (S/N) manifested variations between $30 - 50$ in the Hα continuum region. In the spectroscopic observations of W UMi, Vega (A0V) and α Boo (K1.5 III) were selected as the standard stars for the hotter primary and cooler secondary companions, respectively. According to atmospheric conditions, exposure times between 2500 and 3300 s were given for a total of 16 spectra obtained. For the data reduction, we utilized the ECHELLE task of IRAF code, including the following steps: light subtraction from background, division by a flat field obtained by a halogen lamp, wavelength calibration with the spectrum of a Th-Ar lamp and normalization of the spectra to the continuum.

3 SPECTROSCOPIC ANALYSIS

3.1 RV Measurements and Orbital Properties

In the spectroscopic studies by Sahade (1945) and Joy & Dustheimer (1935), merely the RV measurements of the primary component were determined. W UMi was known as a single-lined binary until the study of Park et al. (2018),

who measured the RV values of both companions and reported orbital parameters. In order to test the orbital parameters found by Park et al. (2018), we aimed to calculate the orbital solution using our own data by measuring RVs of both components with many more absorption lines.

The RV measurements of W UMi were made by executing the IRAF task FXCOR which includes the cross-correlation technique, commonly implemented for this aim. RVs of the hotter, primary component and cooler, secondary component were calculated from 12 and 11 spectra, respectively. We eliminated two spectra from the 16 spectra due to large errors while the RVs were designated for the primary component. The standard stars Vega (A0V, RV $= -13.9$ km s^{-1}) for the primary star and α Boo (K1.5III, RV $= -5.9$ km s^{-1}) for the secondary star were selected as templates for application of the cross-correlation method. Na I D2 and Hα lines were excluded in the spectroscopic analysis in order not to be affected by mass transfer and/or magnetic activity. Furthermore, we did not consider the regions affected by telluric lines. Finally, the wavelength region between 4400 and 6000 Å was preferred to measure RV values of the hotter and cooler companions.

The RVs of the components and their errors determined from spectroscopic analysis are listed in Table 1. The weighted averages of the RVs were determined from the cross-correlation of each order of W UMi spectra used, with the corresponding order of the spectra of standard stars. Calculation methods for the weighted means of the RVs and their errors can be found in several studies (e.g. Frasca et al. 2000; Soydugan et al. 2007).

The secondary component is dimmer than the primary component in the W UMi system. Therefore, the error values of the RVs of the secondary component were found to be larger. The error values computed from RV measurements are approximately 5 km s^{-1} and 10 km s^{-1} for the hotter and cooler components, respectively. The accordance of observational points with theoretical curves is presented in Figure 1. The spectroscopic orbital parameters given in Table 2 were utilized as input parameters in the simultaneous analysis of light and RV curve data. According to the orbital parameters, it is clear that the semi-amplitude for the RV changes in the secondary component ($K_2 \approx 197 \pm 3$ km s^{-1}) and mass ratio of the companion stars ($q = 0.460$) were ascertained to be different from those published by Park et al. (2018).

Table 1 RVs and Their Errors for Hot and Cool Components of W UMi

HJD 24 50000+	Orbital Phase	V_1 (km s^{-1})	V_2 (km s^{-1})
3160.4684	0.0183	–	7.6 ± 11.5
3126.5094	0.0558	–	58.4 ± 12.8
3155.4744	0.0826	-58.3 ± 4.3	90.9 ± 9.7
3167.5015	0.1527	-89.7 ± 5.6	–
3184.5565	0.1783	-92.5 ± 4.7	147.3 ± 9.4
3157.5005	0.2737	-113.8 ± 4.3	182.4 ± 13.2
3203.5845	0.3638	-78.9 ± 5.6	–
3125.5839	0.5118	-6.6 ± 2.5	–
3127.5672	0.6776	56.5 ± 4.5	-189.1 ± 12.6
3185.4074	0.6785	64.8 ± 5.2	-192.6 ± 12.3
3202.5581	0.7604	73.4 ± 6.1	-213.5 ± 11.1
3151.5535	0.7778	79.3 ± 6.8	-201.3 ± 10.6
3170.4324	0.8756	54.1 ± 6.6	-160.5 ± 8.3
3124.5607	0.9103	39.8 ± 6.1	-131.0 ± 9.2

Table 2 Orbital Parameters for W UMi

Parameter	Value
T_0 (HJD)	2452500.3960[1]
$P_{\rm orb}$ (d)	1.7011371[1]
V_γ (km s^{-1})	-15.3 ± 1.1
K_1 (km s^{-1})	90.4 ± 1.5
K_2 (km s^{-1})	196.6 ± 2.6
$a_1 \sin i$ (10^6 km)	2.11 ± 0.05
$a_2 \sin i$ (10^6 km)	4.60 ± 0.10
$M_1 \sin^3 i$ ($M_\odot$)	2.85 ± 0.16
$M_2 \sin^3 i$ ($M_\odot$)	1.31 ± 0.06

Notes: [1]Kreiner (2004).

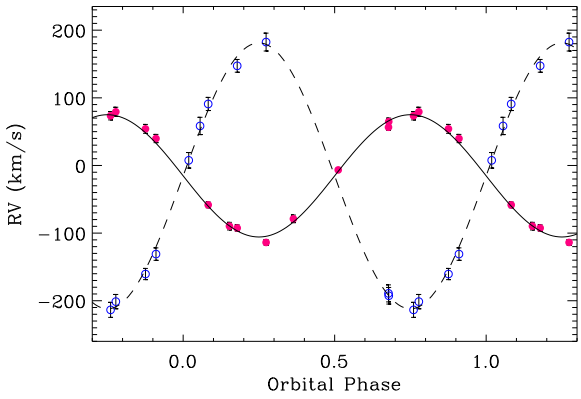

Fig. 1 RV variations of components of W UMi versus orbital phase. RV values of the primary and secondary stars are signified by *filled* and *open circles*, respectively.

3.2 Model Atmosphere Application

In order to model the spectra of W UMi, especially the dominant more massive, hotter companion, the observed spectrum at the orbital phase of about 0.5 was considered. We preferred the spectrum given by Park et al. (2018) s-

ince the spectrum is around the secondary minimum and also has higher resolution. It is almost impossible to determine the atmospheric properties of the cooler secondary companion of W UMi because of its low light contribution ($5\% - 10\%$) to the total light of the target in the optical region.

Our main goal in the spectral synthesis was primarily to test whether the metallicity of the primary component is different from that of the Sun since binary evolution models indicate that the system is rich in metal as described in Section 6.

For modeling of the spectrum, the code `Spectroscopy Made Easy` (`SME`) was chosen (Valenti & Piskunov 1996). The software can be used for fitting the observed spectrum with the spectral synthesis method. Atmospheric parameters of the hotter component of W UMi were determined by interpolation of the ATLAS model atmospheres (Kurucz 1993) included in `SME` software. We have utilized the line information from the Vienna Atomic Line Database (VALD; Piskunov et al. 1995). The spectral region $4460 - 4560$ Å, including several absorption metallic lines and also Hα line, was applied. The temperature ($T_{\rm eff,1} = 9310 \pm 90$ K) and projected rotational velocity ($v_1 \sin i = 107 \pm 5\,{\rm km\,s^{-1}}$) of the hotter companion were derived. During the model atmosphere analysis, the value of surface gravity of the primary component ($\log g_1 = 3.83 \pm 0.02$), which was calculated from the results obtained from the simultaneous analysis of the light and RV curves, was taken as constant in order to avoid parameter degeneration. All atmosphere parameters were found to be in accordance with the values given by Park et al. (2018). On the other hand, although Park et al. (2018) performed spectral analysis under the assumption of solar metallicity, our results displayed higher metallicity than the Sun for the system.

Iron content was used to estimate metallicity of the primary component since the [Fe/H] ratio is easy to measure in the optical spectra. We measured the [Fe/H] ratio to be about $+0.5 \pm 0.2$ from the spectra obtained at the orbital phase of about 0.5 (HJD 245284.3062) by Park et al. (2018). The measured [Fe/H] ratio was converted to metallicity (Z) value as $Z \approx 0.05$. Comparison between the observed spectrum of W UMi and the synthetic spectrum for solar metallicity and $Z = 0.05$ can be seen in Figure 2. This Z value indicates that the primary companion may be a metal-rich star compared to the Sun, which coincides with the evolution models in this study.

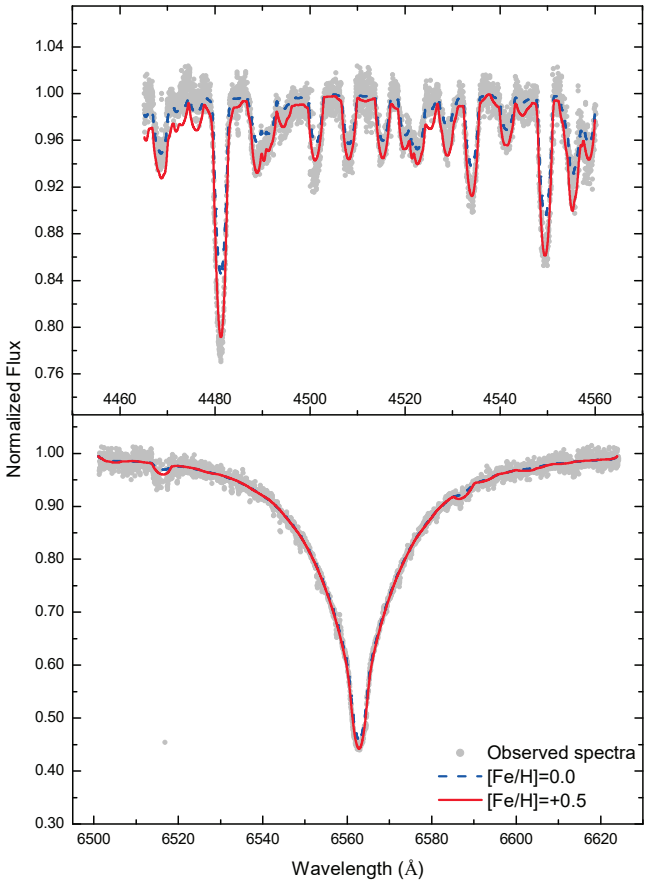

Fig. 2 Synthetic spectrum calculated by `SME` for [Fe/H]$= 0.0$ (*blue dashed line*) and [Fe/H]$= +0.5$ (*red solid line*) together with the observed spectrum (*gray dots*) in wavelength region $4460 - 4560$ Å (*upper panel*) and around region of Hα line (*bottom panel*) (*Color version is online*).

4 SIMULTANEOUS SOLUTION OF BVR LIGHT AND RV CURVES

The RV values of the companions and multi-color LCs of W UMi acquired in this study were simultaneously analyzed by the Wilson-Devinney (WD) code (Wilson & Devinney 1971). All magnitude values obtained from observations in B, V and R bands were normalized to unity around the orbital phase of 0.25. In the WD solution, we used 2930, 2905 and 2890 observational points in B, V and R filters, respectively. All observational points were of the same weight during the analysis. In order to decide accurate MOD in the solution, firstly, we tried the MOD2 given for detached systems. As the surface potential of the less massive, secondary star reached its Roche limit, the analysis was continued and the process was completed with MOD5 corresponding to semi-detached systems.

During the solution, we fixed some parameters as constant while others were set free. Fixed parameters were the

limb-darkening coefficients from van Hamme (1993), the values of bolometric albedos as 1.0 and 0.5 from Ruciński (1969), the gravity darkening coefficients for radiative atmospheres to be 1.0 from von Zeipel (1924) and for convective atmospheres they were 0.32 from Lucy (1967). The rotational parameters (F_1) and (F_2) of both two components were selected as 1.0, assuming synchronous rotation for both companions. A circular orbit ($e = 0$) was accepted as obtained from the solution of the spectroscopic orbit. The free parameters were the inclination (i) of the system's orbit, temperature of the cooler, secondary (T_2), surface potential of the hotter, primary (Ω_1), phase shift, mass ratio (q), semi-major axis (a) of the orbit, RV (V_γ) of the system's mass center and the fractional value of the primary luminosity (L_1) during iterations.

In the analysis, the leading parameters were the temperature of the hotter star and mass ratio of the companion stars. The temperature of the more massive, primary companion was chosen to be 9310 K as reported by Park et al. (2018), which is tested in this study by applying spectral synthesis around the Hα line region and also in the wavelength range $4460 - 4560$ Å. Because of the difference between the spectroscopic mass ratio obtained in this study and the q value determined by Park et al. (2018), photometric q-search was performed employing the light curvesLCs obtained in this study. As a result of this scanning, the minimum value of $\sum(O\text{-}C)^2$ (the weighted sum of the squared residuals) was obtained around $q = 0.44$, which is close to the spectroscopic q value in this study. Therefore, the mass ratio value (q) of 0.460 listed in Table 2 and obtained from the orbital solution was utilized as the input parameter in the solution. In the results of the photometric modeling, the mass ratio obtained was 0.447, which is very close to the spectroscopic mass ratio value.

In order to test the third light contributing to the total light of W UMi, a third light parameter (l_3) was chosen as a free parameter. The third light was accepted to be zero during the iterations since a meaningful value was not obtained for l_3. The physical and geometrical parameters derived from simultaneous analysis of the RVs and multicolor LCs are listed in Table 3. Comparisons of observational points and model curves are displayed in Figure 3. Roche lobes together with the binary demonstrate, in accordance with parameters determined from the analysis of BVR LCs, that while the secondary component fills the Roche lobe, the primary companion fills about 85% of its inner lobe (see Fig. 7). Although W UMi is classified as a classic Algol-type EB, it is a candidate showing characteristics of a near contact semi-detached binary system,

Table 3 Parameters Derived from Analysis of BVR Multi-color LCs and RV Data for W UMi

Parameter	Value
a ($R_\odot$)	10.01(6)
V_γ (km s^{-1})	–15.05 (1.2)
i (°)	83.57(18)
T_1 (K)	9310^a
T_2 (K)	5240(30)
Ω_1	3.266(16)
Ω_2	2.773
Phase shift	0.0001(1)
q	0.447(5)
$L_1/(L_1+L_2)$	0.947(8) (B)
	0.920(5) (V)
	0.895(3) (R)
$L_2/(L_1+L_2)$	0.053 (B)
	0.080 (V)
	0.105 (R)
r_1 (mean)	0.363(1)
r_2 (mean)	0.309(1)

Notes: ^{a}Adopted from Park et al. (2018).

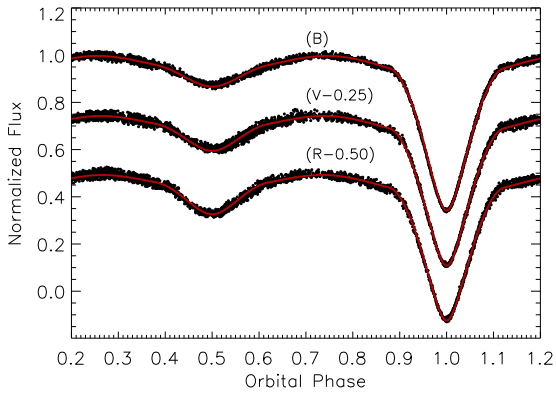

Fig. 3 BVR LCs of W UMi along with theoretical fits.

according to results in Table 3 and also Roche geometry in Figure 7.

5 ORBITAL PERIOD VARIATIONS

Classical Algol-type EB stars or SDBs may indicate changes in their orbital periods with different forms. This can be seen for many systems in the $O - C$ catalog of EB systems (Kreiner et al. 2001). Some SDBs show upward or downward parabolic changes together with cyclic variations or not, although an increase in the orbital period can be expected due to their evolutionary status. This reveals that different physical processes (e.g. mass loss and/or transfer, magnetic activity, existing unseen components) can be effective at the same time or some can be more dominant from time to time.

In this study, the orbital period behavior of semi-detached binary W UMi was studied over a time interval

Table 4 Obtained Minima Times in This Study for W UMi

JD. Hel.+2400000	Error	Min.	Filters
56046.4245	0.0008	II	BVR
56051.5146	0.0006	II	BVR
56052.3721	0.0002	I	BVR

of about a century. In addition to three minima times obtained in this study which are provided in Table 4, 201 eclipse times (172 visual (v), 2 photographic plate (p) and 27 photoelectric (pe) and CCD) were included in the analysis. The data were referenced from the "O-C Gateway" (`http://var2.astro.cz/ocgate/`) and the literature. In this study, analysis was carried out based on $O-C$ data as conducted for many EBs (e.g. Soydugan et al. 2011; Zasche et al. 2008; Yang 2013).

As noted by Kreiner et al. (2008), parabolic and cyclic changes in the $O-C$ graph of the target system are clearly seen. Therefore, the $O-C$ data represent a cyclic term superimposed on a parabola. A secular decline in the orbital period of semi-detached binaries does not coincide with the evolutionary status of these systems since their less massive components are filling their Roche lobes and transferring their mass to the hotter, more massive companion. However, the dominant mechanism may be mass and angular momentum loss from the binary. The cyclic variation can be the result of a tertiary star in the close pair or the magnetic cycle of the secondary component with convective outer layers. These two possible mechanisms were evaluated in this study to interpret cyclic changes in the $O-C$ diagram.

Firstly, $O-C$ data of W UMi is represented by a downward parabola plus light-time effect (LITE) using the following equation

$$T = T_0 + E \times P + Q \times E^2 + \Delta t\,, \qquad (1)$$

where T_0 (reference time for primary eclipse) and P (orbital period) are the light elements of W UMi, while the time delay resulting from an unseen star in the close binary is represented by Δt. The LITE equation, described as a time delay and given by Irwin (1959), is commonly utilized for the analysis of changes in orbital period (e.g. Soydugan et al. 2003, 2006; Zasche et al. 2014).

The parameters derived from the analysis applying the quadratic term and LITE to $O-C$ data are reported in Table 5. Distribution of $O-C$ values, applied model fits and also residuals from the theoretical representation are indicated versus years and also epoch numbers in Figure 4. LITE parameters in Table 5 signify that W UMi has an eccentric orbit around the mass-center of the triple system

Table 5 Parameters and Their Errors Obtained from Analysis of $O-C$ Data for W UMi

Parameter	Value
T_0 (HJD+2400000)	43392.4858(43)
$P_{\rm orb}$ (d)	1.7011469(5)
Q (d)	–6.15(1)$\times 10^{-10}$
$a_{12}\sin i'$ (AU)	2.99(0.65)
e'	0.31(10)
ω' (deg)	189(28)
T' (HJD+2400000)	34867(1526)
P_{12} (years)	71.1(5.7)
$f(M_3)$ ($M_\odot$)	0.0052878(158)
M_3 ($M_\odot$) for $i'=90^\circ$	0.49
K_{12} (km s^{-1})	1.3

with a period of ≈71 yr. The projected distance of the close binary's mass center to the mass-center of the triple system ($a_{12}\sin i'$) was calculated as 2.99 AU. These values of the two parameters allow us to estimate the mass function of the possible tertiary star to be $f(M_3) \approx 0.0053\,M_\odot$. Therefore, the minimum mass of the unseen companion was calculated to be $0.49\,M_\odot$. The amplitude of RV changes of the mass-center of W UMi, relative to that of the third-body system, would be $2.6\,{\rm km\,s^{-1}}$, which can be detectable spectroscopically if spectra can be obtained with a high resolution and high S/N. We found the maximum angular separation between the tertiary component and the close binary to be approximately $0''.12$ for a distance of 414 pc which was taken from the Gaia-DR2 database (Gaia Collaboration et al. 2016, 2018).

Cyclic $O-C$ changes for W UMi can be also interpreted as possible magnetic activity on the surface of the cooler companion. Applegate (1992) proposed a model to interpret this type of variation in the periods of close binaries, which was applied to many active close binaries, including at least one star with an outer convective envelope. We employed the basic sinusoidal equation to model the cyclic changes of the $O-C$ values of the target as applied to many active binary stars (e.g. Tian et al. 2009; Zhang et al. 2019). Applying the method of differential correction, the parameters of the sinusoidal changes were derived and are listed in Table 6, together with the Applegate model's parameters. The rate of the modulation period, resulting from the magnetic cycle of the cooler, less massive star in the system, was calculated as $\Delta P/P \approx 5.5\times10^{-6}$, while the average sub-surface magnetic field of the companion of late spectral type was estimated to be ≈2.7 kG. The model parameters in Table 6 for W UMi were found to be consistent with those proposed by Applegate (1992).

The value of the quadratic term (Q) is indicative of a decline in the period of the target, with a rate of $dP/dt = -1.55\times10^{-7}\,{\rm yr^{-1}}$ due to mass loss from the close bi-

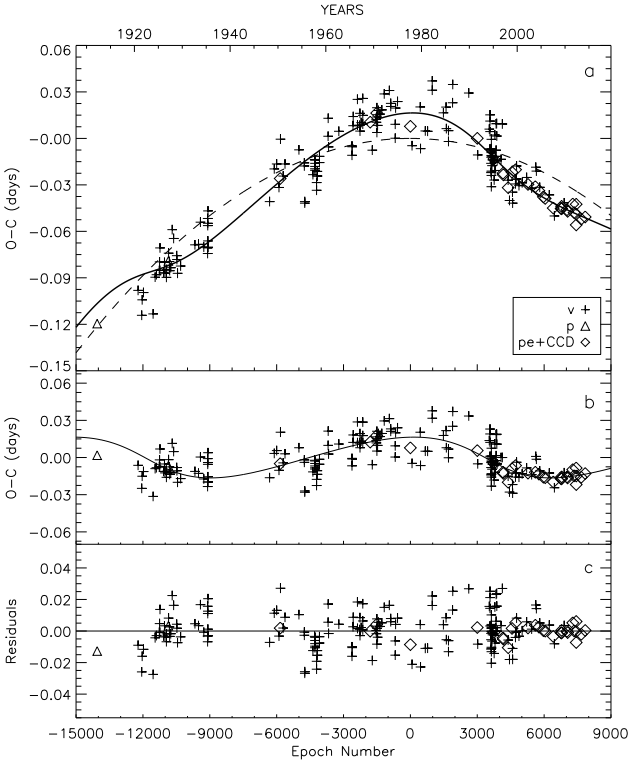

Fig. 4 (a) Variation of $O-C$ values of W UMi fitted with a parabolic term (*dashed line*) and parabolic plus LITE (*solid line*) fit. (b) LITE representation of $O-C$ data after removing parabolic term. (c) Residuals from theoretical representation.

Table 6 Parameters of Sinusoidal $O-C$ Change and Applied Applegate Model for Cooler Companion in W UMi

Parameter	Value
T_0 (HJD+2400000)	43392.4841(54)
$P_{\rm orb}$ (d)	1.7011525(6)
T_s (cycle)	3789(30)
$A_{\rm mod}$ (d)	0.016(3)
$P_{\rm mod}$ (d)	25385(75)
ΔP (s)	0.582
$\Delta P/P$	4.0×10^{-6}
ΔJ (g cm^2 s^{-1})	8.3×10^{47}
I_s (g cm^2)	8.9×10^{54}
$\Delta\Omega/\Omega$	0.0015
ΔE (erg)	1.6×10^{41}
$\Delta L_{\rm rms}$ (erg)	2.2×10^{32}
B (kG)	2.7
Δm (mag)	0.0006

nary. Under the assumption of mass transfer from the less massive component to the more massive one at a rate of $10^{-8}\,M_\odot$ yr^{-1} due to the semi-detached status of W UMi, the amount of mass escaping from the system can be estimated to be $dM/dt = -5.8\times10^{-8}\,M_\odot$ yr^{-1}. The calculation method for the rates of mass loss, together with mass transfer in the system, can be referenced in the study of Soydugan et al. (2011).

Table 7 Main Physical Parameters of W UMi

Parameter	Primary	Secondary
Mass ($M_\odot$)	3.22 ± 0.08	1.44 ± 0.05
Radius ($R_\odot$)	3.63±0.04	3.09 ± 0.03
Temperature (K)	9310 ± 90^a	5240 ± 200
$\log L$ ($L_\odot$)	1.95 ± 0.03	0.81 ± 0.08
$\log g$ (cgs)	3.83 ± 0.02	3.62 ± 0.02
$M_{\rm bol}$ (mag)	-0.13 ± 0.06	2.71 ± 0.15
BC (mag)	-0.24^b	-0.35^b
M_v (mag)	-0.01 ± 0.09	2.92 ± 0.15
$E(B-V)$ (mag)	0.10	
Orbital separation ($R_\odot$)	10.01 ± 0.06	
Photometric distance (pc)	422±40	
Gaia DR2 distance (pc)	414±5	

Notes: ^{a}Park et al. (2018), ^{b}Drilling & Landolt (2000).

6 ABSOLUTE PROPERTIES AND EVOLUTIONARY STATUS

The fundamental astrophysical parameters of the semi-detached binary W UMi were determined with the simultaneous solution of BVR multi-color LCs and the RV data of the companion stars. Although W UMi is classified as an SDB, a cooler, less massive star fills its Roche volume as expected, but another hotter component fills about 85% of its Roche lobe according to the photometric solution. Therefore, the system should be considered as a near-contact semi-detached binary. The absolute parameters, which were computed using the parameters listed in Table 3, are shown in Table 7. The bolometric correction values of the companions applied in the calculation were chosen from Drilling & Landolt (2000) with a solar temperature ($T_{\rm eff,\odot}$) of 5777 K and solar bolometric magnitude ($M_{\rm bol,\odot}$) of 4.74 mag.

From the simultaneous solution of the RVs of the companions and multi-color photometric data, the mass and radius of the hotter primary star were calculated to be 3.22±0.08 $M_\odot$ and 3.63±0.04 $R_\odot$, respectively. The designated mass value corresponds to the B8 spectral type according to the absolute parameters of main sequence stars by Eker et al. (2018). The radius value of the primary component was identified as being fairly large for the B8 spectral type. The $\log g$ value of the secondary star and its other basic parameters indicate that it is a distorted sub-giant star, as confirmed by photometric results.

The photometric distance of W UMi was ascertained to be 422±40 pc using the absolute parameters and interstellar reddening given in Table 7. We estimated the value of the color excess, $E(B-V)$ value to be $\approx 0^{\rm m}.10$ from the Galactic extinction maps of Schlegel et al. (1998). The calculated distance is compatible with the value, 414±5 pc,

provided by the Gaia DR2 database (Gaia Collaboration et al. 2018) within error limits.

We also calculated the components of space velocities (*U,V,W*) based on the proper motions and parallax value from the Gaia DR2 database (Gaia Collaboration et al. 2018), and also the velocity of the center of mass of the system from this study. Differential corrections for the space velocities were calculated applying the formulas given by Mihalas & Binney (1981), while the corrections for the local standard of rest were according to the study of Coşkunoğlu et al. (2011). The corrected space velocity values were found to be (*U,V,W*) = $(-27.9 \pm 0.7, -16.6 \pm 0.9, -2.2 \pm 1.2)$ km s^{-1}, while the total space velocity of W UMi was calculated as 32.5 ± 1.7 km s^{-1}. The basic kinematic characteristics of the system indicate that it may be a member of the thin disk of our Galaxy, according to the criteria of Leggett (1992).

In order to investigate the evolutionary states of the NCB W UMi, binary evolutionary models were generated with version 8845 of `Module for Experiments in Stellar Astrophysics` (`MESA`) code using the binary module (Paxton et al. 2011, 2013, 2015, 2018). Models were constructed under two different approaches (conservative and non-conservative mass transfer) and also the different initial values of the components' masses (M_{1-i} and M_{2-i}), initial orbital period of the system ($P_{\rm orb-i}$) and also metallicity (Z). Thus, a large number of models were produced in order to search for compliance with the observed parameters of the system. During the model generation process, the initial mass varied between 2.35 and 2.95 $M_\odot$ for the primary component and between 2.35 and 4.45 $M_\odot$ for the secondary component, while we changed the initial value of the orbital period from 1.3 to 2.3 d. The metallicity value was also altered from $Z = 0.01$ to $Z = 0.06$ for both the conservative and non-conservative models. We also used parameter α, meaning the fractional mass loss from the system in the vicinity of the secondary component as defined by Soberman et al. (1997), as a variable during calculations for the non-conservative models. In addition, the effect of magnetic braking (Rappaport et al. 1983) was also included in the model's calculations by considering the current mass of the cooler component in order to take into account the angular momentum change of the system during evolution. Applications of the binary module of `MESA` code to reveal the evolutionary state of binary stars can be found in several studies, which includes information on model calculations and explanations of the used parameters (e.g. Paxton et al. 2015; Streamer et al. 2018; Rosales et al. 2019).

Table 8 Evolutionary Model Parameters Derived From `MESA` for W UMi

Mass transfer modes	Z	M_{1-i} ($M_\odot$)	M_{2-i} ($M_\odot$)	$P_{\rm orb-i}$ (d)	Age (Myr)
Conservative	0.014	2.36	2.35	2.29	520
Conservative	0.055	2.29	2.41	3.10	880
Non-conservative	0.055				
$\alpha = 0.1$		2.29	2.52	2.98	790
$\alpha = 0.3$		2.37	2.73	2.81	660
$\alpha = 0.5$		2.47	3.01	2.63	530
$\alpha = 0.7$		2.60	3.62	2.27	400
$\alpha = 0.9$		2.95	4.45	1.33	280

The possible binary star evolution models, which we can implement to explain the evolutionary status of W UMi, were investigated comparing the surface gravity ($\log g$) and radii of the companions from the models and analysis of observational data. Model parameters from `MESA` are listed in Table 8, which are assumed under the approaches of conservative and non-conservative mass transfer. As seen from the table, we calculated models for solar metallicity ($Z = 0.014$) and also for metal-rich mode with $Z = 0.055$, which yields a better match with the parameters of the target derived from analysis of the observations. In Figure 5, the locations of both companions of the system in the diagram of $\log L - \log T_{\rm eff}$ together with the evolutionary models from the `MESA` binary module with solar metallicity and also $Z = 0.055$ were produced under the assumptions of conservative and non-conservative evolution. It can be seen from Figure 5(a) that the models produced for solar metallicity do not show good compatibility with the current properties of the companions of W UMi. Figure 6 indicates the radii variations and also mass-luminosity relations of the components during non-conservative evolution for $Z = 0.055$. Evolutionary tracks in Figures 5 and 6 were generated by `MESA` for the initial masses of the components in Table 8.

In the non-conservative approach, models were produced for different values of the fractional mass loss parameter (α). The best match with the current parameters of the system was $\alpha = 0.7$. In that case, the system's age was estimated as ≈ 400 Myr, while conservative models with $Z = 0.055$ give an age of ≈ 880 Myr.

7 DISCUSSION AND CONCLUSIONS

SDB type binaries are valuable for investigation of the evolutionary phases of close binaries and the processes affecting evolution, such as mass transfer and loss. On the other hand, it is not easy to obtain the absolute parameters of

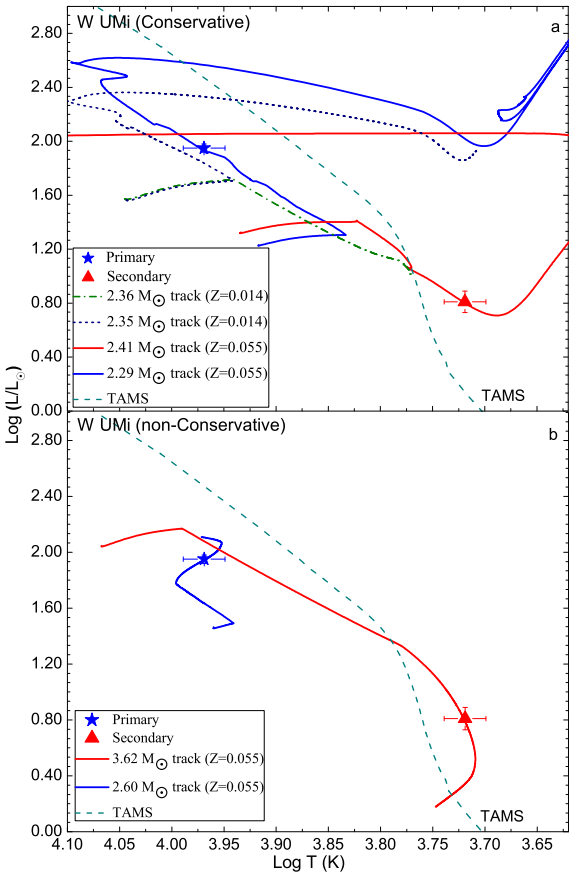

Fig. 5 Positions of primary and secondary components of W UMi represented by *filled star* (primary) and *triangle* (secondary) in the plane of $\log L - \log T_{\rm eff}$. *Dashed lines* indicate Terminal Age Main Sequence (TAMS). Under the conservative mass transfer approach, evolutionary tracks for obtained initial masses according to metallicities Z $= 0.014$ (*dot-dashed line* for primary, *dotted line* for secondary) and Z $= 0.055$ (continuous *blue line* for primary and *red line* for secondary) are displayed in the upper panel (a). In the bottom panel (b), evolutionary tracks calculated under the non-conservative mode for primary (*red line*) and secondary (*blue line*) components are drawn for Z $= 0.055$. All theoretical curves were calculated by MESA.

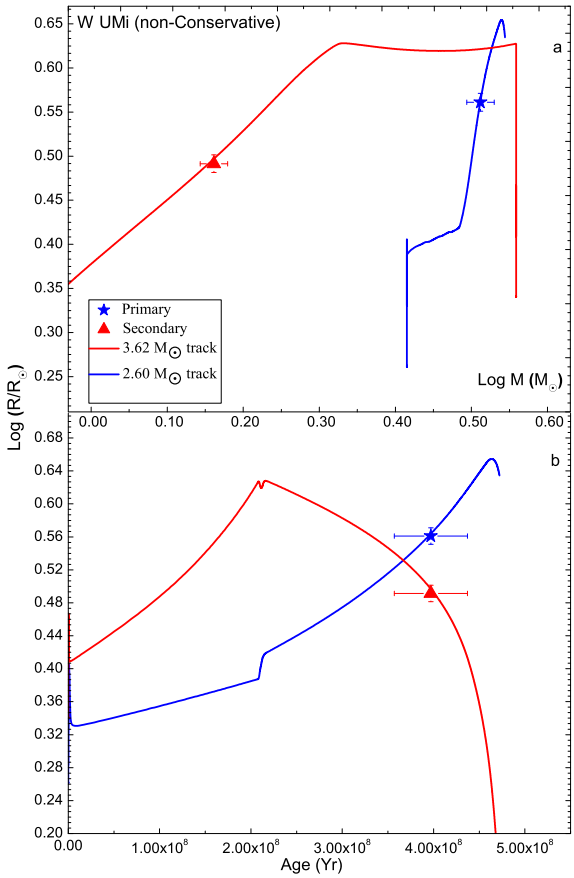

Fig. 6 Locations of primary (*filled star*) and secondary (*filled triangle*) companions of W UMi in planes of $\log R - \log M$ and $\log R$ – Age in upper (a) and lower (b) panels, respectively. Evolutionary calculations for primary companion with initial mass of 2.60 $M_{\odot}$ (*blue line*) and secondary companion with initial mass of 3.62 $M_{\odot}$ (*red line*) were made for the non-conservative mass transfer mode. All theoretical curves were calculated by MESA.

these systems due to faint secondaries in the optical region and also mass transfer and loss events. In the catalog by Ibanoğlu et al. (2006), there are only 38 eclipsing double-lined SDBs, and so far the number of these systems has not greatly increased, although many optical LCs of the SDBs have been gained from several ground-based surveys (e.g., ASAS, SuperWASP) and satellites (e.g. *Hipparcos*, *Kepler*, *TESS*).

W UMi is a double-lined semi-detached binary and is also close to the contact phase, as indicated by recent analysis. The target can therefore be classified as a near-contact, semi-detached binary based on the description of Zhu & Qian (2009) because the hotter component appears to fill approximately 85% of its inner Roche lobe. It is worthwhile studying W UMi from this aspect and the reasons are as follows: i) to derive the main absolute parameters of the companion stars based on both spectroscopic and photometric analysis, ii) to investigate its orbital period variation, and iii) to examine the evolution of the system by producing binary evolution models under both the conservative and non-conservative mass transfer approaches.

The simultaneous analysis of LCs and RV data produces a mass ratio value ($q = 0.447 \pm 0.005$) greater by $\sim$8% than the value given by Park et al. (2018), which is due to the different measurements of RV data of the components. Therefore, it can be said that the mass of the primary component is found to be smaller but its radius is larger, when we compare them with the values of Park et al. (2018). The errors calculated for the masses

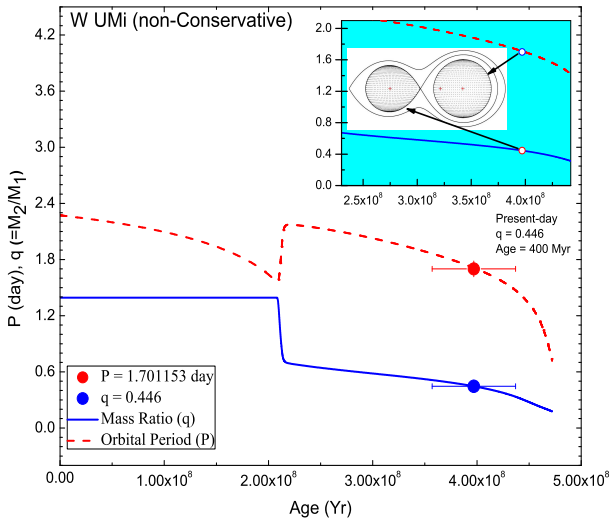

Fig. 7 Variation of orbital period (P) and mass ratio (q) of W UMi versus its age until system reaches contact phase. Position of the system based on present P and q values, and also current Roche geometry (inner box) are indicated. Theoretical lines were drawn using MESA binary models.

and radii of both components are on the order of 3% and 1%, respectively. From the spectral synthesis analysis, it may be suggested that the system has a higher metallicity ([Fe/H]$\approx 0.5 \pm 0.2$) than the Sun, as is apparent in Figure 2, although solar metallicity was assumed by Park et al. (2018). The metal-rich state of the system is supported by the fact that it is a thin-disk member, as derived from kinematic analysis as well as by binary evolution models. The surface gravity values of the cooler companions indicate that it is a sub-giant star. The hotter, primary component has a lower $\log g$ value than values of main-sequence stars with the same spectral type and mass (e.g., Eker et al. 2018). The mass of the gainer component is found to be larger than that of main sequence stars at the same temperature, which is most likely due to the evolutionary state of the target and the mass loss and transfer process, as seen in the generated evolutionary models.

Mass transfer in classical SDBs takes place from the less massive component to the more massive star. Therefore, the orbital period of these systems is expected to increase. In the case of W UMi, the orbital period was found to be decreasing at a rate of $-0.02\,\mathrm{s\,yr^{-1}}$ when we analyzed minima times reported in the last century. The decrease in the period may occur due to mass loss from the system ($5.8\times10^{-8}\,M_\odot\,\mathrm{yr}^{-1}$). In addition to the secular changes, the $O-C$ values of the target also manifest a cyclical change, which can be interpreted as a possible third body or magnetic activity on the surface of the active component (e.g., Soydugan et al. 2003; Zasche et al. 2010). In this study, LITE analysis indicated that a tertiary companion around the close pair with a minimum mass of $\approx 0.49\,M_\odot$ and a period of 71 yr may cause this kind of cyclic $O-C$ variation. On the other hand, a significant third light (l_3) could not be determined during the analysis. In this study, the parameters obtained by applying parabolic and LITE terms to the $O-C$ values in general are compatible with those obtained by Kreiner et al. (2008), but various values have been found to be above the error level for some parameters (e.g., mass and orbital period of a possible third body). Magnetic activity of the sub-giant companion with a temperature of 5240 K may be the cause of such cyclic variations in the $O-C$ diagram. Therefore, the Applegate model was also utilized to explain the cyclic period variations of W UMi and the calculated model parameters were found to be compatible with those proposed in Applegate (1992).

In this study, binary evolutionary models were propagated by MESA code to try to understand the present evolutionary status and to investigate the initial state of the system. Both conservative and non-conservative mass transfer approaches were implemented for solar metallicity and also for the system having higher metallicity than the Sun. Although the conservative models with Z$=0.05$ are not far from representing the observational parameters of the target system, a better fit with the observational data was achieved in non-conservative models with $Z=0.05$ values. In some studies, it was reported that non-conservative models better represent the observational parameters of classical Algols (e.g., Sarna 1993; van Rensbergen et al. 2011). The decreasing orbital period of W UMi determined by $O-C$ analysis, which can also be seen for several Algols (e.g., Qian 2002; Soydugan et al. 2011), may also be considered as evidence to support non-conservative evolutionary models.

In the most compatible evolutionary models in non-conservative mode, the age of W UMi could be ≈400 Myr with an initial orbital period of 2.3 d, as ascertained in Table 8. Important transition points for the evolution were also examined during the model calculations. The best non-conservative model matching the observed data suggests that the first Roche-lobe overflow (RLOF) started when the age of the target was ≈200 Myr and it had an orbital period of ≈1.4 d. The mass transfer rate in the system was calculated to be $1\times10^{-7}\,M_\odot\,\mathrm{yr}^{-1}$ during the first RLOF phase. In Figure 7, variation of the orbital period (P) and mass ratio (q) of the companion stars can be viewed during evolution until the contact phase. In addition, the current P and q values are indicated together with

the present Roche geometry in Figure 7. Non-conservative binary models show that the near-contact system W UMi may be a contact binary after about $40 - 50$ Myr. It is estimated from the models that the values of P and q of the system will decrease until the contact phase (Fig. 7) and when it reaches the contact phase, the orbital period and mass ratio will be ≈1.4 d and ≈0.3, respectively.

From the results in this study and also the literature, it is thought that investigation of W UMi type near-contact semi-detached systems is important to understand the nature of these binaries and also possible transition from semi-detached status to the contact phase during the evolution of close interacting binary stars. In the case of W UMi, more spectroscopic data with high-resolution and S/N is needed to reliably derive the metal abundance of the system, to obtain clues on its mass flow and loss processes and to check the possible magnetic cycle of the cooler component and any unseen companion around the binary system.

Acknowledgements This work was supported by Çanakkale Onsekiz Mart University, the Scientific Research Coordination Unit, Project number: FBA-2018–2549 and also partly supported by TÜBİTAK (Scientific and Technological Research Council of Turkey) under Grant No. 111T224. The authors wish to thank the all staff of the Catania Astrophysical Observatory for the allocation of telescope time and help during observations. This research made use of VizieR and SIMBAD databases at CDS, Strasbourg, France. We are grateful to Dr. Jang-Ho Park for providing us with spectral data on the system. This work has made use of data from the European Space Agency (ESA) mission *Gaia* (`https://www.cosmos.esa.int/gaia`), processed by the *Gaia* Data Processing and Analysis Consortium (DPAC, `https://www.cosmos.esa.int/web/gaia/dpac/consortium`). Funding for the DPAC has been provided by national institutions, in particular the institutions participating in the *Gaia* Multilateral Agreement.

References

Applegate, J. H. 1992, ApJ, 385, 621
Astbury, T. H. 1913, Astronomische Nachrichten, 194, 413
Coşkunoğlu, B., Ak, S., Bilir, S., et al. 2011, MNRAS, 412, 1237
Drilling, John S. & Landolt, A. U., 2000, Allen's Astrophysical Quantities, 4th ed., Edited by Arthur N. Cox (New York: AIP Press, Springer)
Devinney, Edward J., J., Hall, D. S., & Ward, D. H. 1970, PASP, 82, 10
Djurašević, G., Rovithis-Livaniou, H., Rovithis, P., et al. 2003, A&A, 402, 667
Eker, Z., Bakış, V., Bilir, S., et al. 2018, MNRAS, 479, 5491
Frasca, A., Marino, G., Catalano, S., & Marilli, E. 2000, A&A, 358, 1007
Gaia Collaboration, Brown, A. G. A., Vallenari, A., et al. 2016, A&A, 595, A2
Gaia Collaboration, Brown, A. G. A., Vallenari, A., et al. 2018, A&A, 616, A1
Ibanoğlu, C., Soydugan, F., Soydugan, E., & Dervişoğlu, A. 2006, MNRAS, 373, 435
Irwin, J. B. 1959, AJ, 64, 149
Joy, A. H., & Dustheimer, O. L. 1935, ApJ, 81, 479
Kaitchuck, R. H., & Honeycutt, R. K. 1982, PASP, 94, 532
Kreiner, J. M. 2004, Acta Astronomica, 54, 207
Kreiner, J. M., Kim, C.-H., & Nha, I.-S. 2001, An Atlas of O-C Diagrams of Eclipsing Binary Stars, Parts 1-6, (Cracow: Pedagogical University Press)
Kreiner, J. M., Pribulla, T., Tremko, J., Stachowski, G. S., & Zakrzewski, B. 2008, MNRAS, 383, 1506
Kurucz, R. L. 1993, Astronomical Society of the Pacific Conference Series, 44, A New Opacity-Sampling Model Atmosphere Program for Arbitrary Abundances, eds. M. M. Dworetsky, F. Castelli, & R. Faraggiana, 87
Leggett, S. K. 1992, ApJS, 82, 351
Lucy, L. B. 1967, ZAp, 65, 89
Mardirossian, F., Mezzetti, M., Predolin, F., & Giuricin, G. 1980, A&AS, 40, 57
Mihalas, D., & Binney, J. 1981, Galactic astronomy. Structure and kinematics (San Francisco: Freeman, 1981, 2nd ed.)
Nakamura, Y., Asada, K., & Sato, R. 1998, Information Bulletin on Variable Stars, 4647, 1
Park, J.-H., Hong, K., Koo, J.-R., Lee, J. W., & Kim, C.-H. 2018, AJ, 155, 133
Paxton, B., Bildsten, L., Dotter, A., et al. 2011, ApJS, 192, 3
Paxton, B., Cantiello, M., Arras, P., et al. 2013, ApJS, 208, 4
Paxton, B., Marchant, P., Schwab, J., et al. 2015, ApJS, 220, 15
Paxton, B., Schwab, J., Bauer, E. B., et al. 2018, ApJS, 234, 34
Payne-Gaposchkin, C. 1952, Annals of Harvard College Observatory, 118, 1
Piskunov, N. E., Kupka, F., Ryabchikova, T. A., Weiss, W. W., & Jeffery, C. S. 1995, A&AS, 112, 525
Qian, S. 2002, PASP, 114, 650
Rappaport, S., Verbunt, F., & Joss, P. C. 1983, ApJ, 275, 713
Rosales, J. A., Mennickent, R. E., Schleicher, D. R. G., & Senhadji, A. A. 2019, MNRAS, 483, 862
Ruciński, S. M. 1969, Acta Astronomica, 19, 245
Sahade, J. 1945, ApJ, 102, 470
Sarna, M. J. 1993, MNRAS, 262, 534
Schlegel, D. J., Finkbeiner, D. P., & Davis, M. 1998, ApJ, 500, 525
Shaw, J. S. 1994, Mem. Soc. Astron. Italiana, 65, 95

Soberman, G. E., Phinney, E. S., & van den Heuvel, E. P. J. 1997, A&A, 327, 620
Soydugan, F., Demircan, O., Soydugan, E., & İbanoğlu, C. 2003, AJ, 126, 393
Soydugan, F., Soydugan, E., İbanoğlu, C., & Demircan, O. 2006, Astronomische Nachrichten, 327, 705
Soydugan, F., Frasca, A., Soydugan, E., et al. 2007, MNRAS, 379, 1533
Soydugan, F., Erdem, A., Doğru, S. S., et al. 2011, New Astron., 16, 253
Streamer, M., Ireland, M. J., Murphy, S. J., & Bento, J. 2018, MNRAS, 480, 1372
Tian, Y. P., Xiang, F. Y., & Tao, X. 2009, Ap&SS, 319, 119
Valenti, J. A., & Piskunov, N. 1996, A&AS, 118, 595
van Hamme, W. 1993, AJ, 106, 2096
van Rensbergen, W., de Greve, J. P., Mennekens, N., Jansen, K., & de Loore, C. 2011, A&A, 528, A16
von Zeipel, H. 1924, MNRAS, 84, 665
Wilson, R. E., & Devinney, E. J. 1971, ApJ, 166, 605
Yang, Y. G. 2013, New Astron., 25, 109
Zasche, P., Liakos, A., Wolf, M., & Niarchos, P. 2008, New Astron., 13, 405
Zasche, P., Uhlář, R., & Svoboda, P. 2010, Ap&SS, 326, 119
Zasche, P., Wolf, M., Uhlař, R., & Kučáková, H. 2014, AJ, 147, 130
Zhang, B., Qian, S. B., Zhi, Q. J., et al. 2019, PASP, 131, 034201
Zhu, L., & Qian, S. 2009, Astronomical Society of the Pacific Conference Series, 404, Photometric Study of Near Contact Binaries, eds. S. J. Murphy, & M. S. Bessell, 189